

# Design of DC / DC bidirectional converter based on DSP in renewable energy

**Abstract.** This article presents a design method for a novel converter. This method can be applied to design DC/DC unidirectional converters and DC/DC bidirectional converters. Also, a new switching technique and the corresponding algorithm are introduced. This algorithm is implemented on a Spectrum Digital eZdsp™ TMS320F2812 card. A laboratory prototype has been built and tested in order to verify the design method and algorithm.

**Streszczenie.** Zaprezentowano metodę projektowania przekształtnika DC/DC. Zaproponowano nową technikę przełączania i odpowiedni algorytm zaimplementowany na procesor TMS320F2812. (Projekt przekształtnika DC/DC bazującego na procesorze sygnałowym z odnawialną energią)

**Keywords:** Bidirectional converter, digital signal, processor, design method.  
**Słowa kluczowe:** przekształtnik dwukierunkowy, procesor sygnałowy

## Introduction

Owing to the raising concern about the environment and a possible energy crisis in the last decade, the potential of renewable energy sources are being recognized and as a result many countries are today actively developing electricity generation systems using renewable energy sources.

An feature of all renewable energy sources is its available energy varies in a random manner, resulting a wide variation in the available output voltage and power, this situation causes the power converter is a necessary part of the generation systems. In a hybrid distribution generation system with battery storage function, as depicted in Fig. 1(a). The dc bus may be connected to a generator [1] driven by a wind turbine through a controlled rectifier. The battery may discharge and charged through the bidirectional dc/dc converter to keep the dc-bus voltage almost constant [2].

Other dc renewable energy sources can be fuel cells [3–5] and photovoltaic arrays [6,7], these can also be connected to the bus with a unidirectional dc–dc converter. Bidirectional dc/dc converter can also find usage in two-quadrant dc motor drives [8]. Among the different types of configurations in high-power applications, the HF isolated dc/dc converter is gaining more attentions due to its high-power density and low cost. Dual-active-bridge converters with HF isolation or Dual-bridge phase-shifted dc/dc converters has been proposed for high-power applications [9,10]. The leakage inductance of the transformer is utilized as the energy transfer device. The net power and the direction of its current is controlled by the phase-shift angle of two bridges located on either sides of a HF transformer. Different modifications on this configuration can also be found in literature [5], [11,12].

This article presents a calculation method and a technique of switching. A novel switching algorithm for a DC/DC converter has been implemented on DSP. This method can be applied to unidirectional and bidirectional converters. Fig. 1 shows these converters, which are elements of a hybrid system.

In order to test the correct operation of the control algorithm of the converters, the MATLAB-Simulink® program was used to model the corresponding algorithm of the converter, which was implemented in a prototype, assembled using a Spectrum Digital eZdsp™ TMS320F2812 card with a DSP F2812.

## Design considerations

The circuits of the full-bridge converters for both bidirectional and unidirectional discussed in this article are

shown in Fig. 1. The maximum duty cycle of the gate voltage should be slightly less than 50% of  $T$ . This type of converter is suitable for high power and high voltage application, since the voltage stress on the switches and diodes does not exceed  $V_{in}$  and  $V_{in}/m$ . In Fig. 1, the diodes connected to each transistor will be identified with the letter  $D$  and the corresponding transistor subscript. During time  $0 < t < DT$ , the switches  $S_1$  and  $S_3$ , and the diodes  $D_6$  and  $D_8$ , are conducting. The voltages across the diodes  $D_2$  and  $D_4$  are  $V_{D4} = V_{D2} = V_{in}$ . Also  $E_1 = V_{in}$ .

For the design of the converter,  $V_o$  and the range of output power values ( $P_{Omax}$ ,  $P_{Omin}$ ) must be established. Taking into account the fixed power and voltage values, the maximum and minimum output current values of the converter are represented as:

$$I_{Omax} = P_{Omax} / V_o \quad I_{Omin} = P_{Omin} / V_o$$

Once the current values are known, we can determine the maximum and minimum load resistance values that can be connected to the converter.

$$R_{Lmax} = V_o / I_{Omin} \quad R_{Lmin} = V_o / I_{Omax}$$

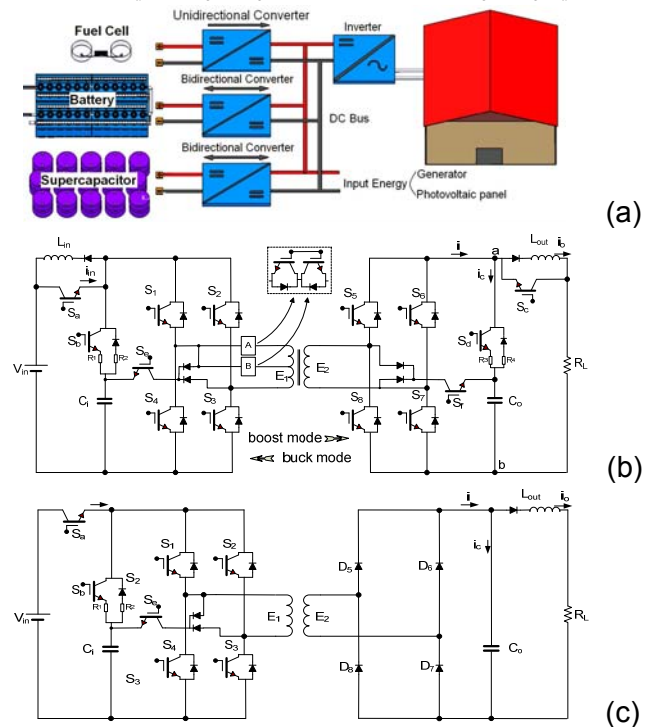


Fig. 1. (a) Hybrid system, (b) Proposed bidirectional converter, (c) Proposed unidirectional converter

In any real voltage source, the supply voltage is variable, so that the three voltage values must be defined. Minimum and maximum values, which are the smallest and largest of the voltage source for normal working conditions, and the nominal voltage value, which is the average value of the voltage source provided in normal working conditions. As the output voltage must be maintained at a fixed value  $V_o$ , we can define three transfer functions.

$$(1) \quad M_{VDCmin} = \frac{V_o}{V_{inmax}} \quad M_{VDCnom} = \frac{V_o}{V_{innom}} \quad M_{VDCmax} = \frac{V_o}{V_{inmin}}$$

The duty cycle of each branch of the converter input can take a maximum value of  $0.5D$ . In order not to use the entire cycle, a value of  $0.4D$  has been considered ( $D_{max}$ ). The efficiency of the converter will be estimated, this estimation can be done without any problem taking a value lower than the real efficiency of the converter. The converter efficiency can be estimated between (0.85 - 0.90).

Using the assumptions related with the efficiency and  $D_{max}$  value, the converter transformer turns ratio is calculated.

$$(2) \quad m = \frac{2\rho D_{max}}{M_{VDCmax}}$$

Taking the value of  $m \leq$  then that obtained in (2). If the converter is bidirectional, the transformer will have two transformer turns ratios, one for the buck converter mode and the other for the boost converter mode. Therefore, a transformer is necessary with two voltage taps. If the voltage difference is not great it's possible to use an autotransformer. The design of the rest of the circuit elements will take into account the maximum power converted and also the direction it will be converted.

Once the transformer turns ratios are fixed, the range of values for the duty cycle as well as its nominal value can be determined.

$$(3) \quad D_{max} = \frac{mM_{VDCmin}}{2\rho} \quad D_{nom} = \frac{mM_{VDCnom}}{2\rho} \quad D_{min} = \frac{mM_{VDCmin}}{2\rho}$$

After setting the switching frequency  $f_c$  at which the converter will work, the switching period  $T=(1/f_c)$  can be determined.

The output filter must have a minimum inductance value, in order to the converter works in continuous conduction mode. So, the inductance value is:

$$(4) \quad (L_{out} \circ L_{in}) \geq (L_{out(min)} \circ L_{in(min)}) = \frac{R_{Lmax} T (0.5 - D_{min})}{2}$$

On the other hand, in order to determine the maximum ripple value of output current, it is also necessary to have the minimum inductance value, which can be obtained by the following expression

$$(5) \quad (L_{out} \circ L_{in}) \geq (L_{out(min)} \circ L_{in(min)}) = \frac{V_o T (0.5 - D_{min})}{\Delta i_{Lout(max)}}$$

Therefore, the value of the inductance of the coil of the filter will be greater or equal to the highest value obtained in expressions (4) and (5). If the converter is bidirectional, then the calculation must be done for the two inductors, the input  $L_{in(min)}$  and the output  $L_{out(min)}$ . With the filter inductance value obtained, the load current ripple value can be determined by:

$$(6) \quad (\Delta i_o) = \frac{V_o T (0.5 - D_{min})}{L_{out}}$$

According to Fig. 1(b), the ripple voltage between nodes "a" and "b" is:  $\Delta v_{ab} = \Delta i_{Lout} (\bar{R}_L + 2\pi f_c L_{out})$ , the imaginary part of impedance is much smaller than the real part, therefore can

be neglected, resulting  $\Delta v_{ab} \approx \Delta i_{Lout} R_L$ . To obtain the  $r_c$  value, it's necessary to find a compromise value. If the  $r_c$  value taken is very small, the currents flowing through the capacitor branches are going to be very large. And if the value of  $r_c$  is very large, this will increase the ripple voltage value. Thus, the expression for determining the resistance of the capacitor is

$$(7) \quad \frac{\Delta V_{ab}}{\Delta i_{o(max)}} = r_{c(max)} \geq r_c \geq r_{c(min)} = \frac{\Delta V_{ab}}{\Delta i_{c(max)}}$$

It is advised that the  $r_c$  value is taken closer to  $r_{cmin}$ , in order to obtain a low ripple as possible, always taking into account of not endangering the circuit components. Therefore, two resistors have been used,  $R_3$  for limiting load current of the capacitor  $C_o$  and  $R_4$  to limit the discharge of  $C_o$ .

In order to determine the minimum value of the filter's capability, with the objective of obtaining the expected ripple, the following expression can be used:

$$(8) \quad C = \left( D \left( 1 - \frac{1}{2} \frac{\Delta i_o}{\Delta i} \right) \cdot \frac{T}{2} \right) / r_c$$

Considering the ripple in the coil is much smaller than the ripple in the capacitor, expression (8) becomes (9). If the converter is bidirectional,  $C_i$  and  $C_o$  are calculated using expression.

$$(9) \quad C \geq C_{min} = \frac{D_{max}}{2f_c r_c}$$

The value used for  $C$  must be greater than  $C_{min}$ .

### Principle of circuit operation

As can be seen in Fig.1 the converter can be designed as bi-directional or unidirectional. The bi-directional is symmetrical and more complex, it can operate in boost mode and buck mode. The duty cycle for both modes is also symmetrical, and therefore due to space limitations, this article will only show the duty cycle and stages of boost mode operation. Fig. 2 shows the duty cycle and Fig. 3 shows the stages of operation.

Before starting the steady state operation the converter must charge the capacitors  $C_i$  and  $C_o$  to prevent the connection transient, for this operations  $S_b$  and  $S_d$  are used.

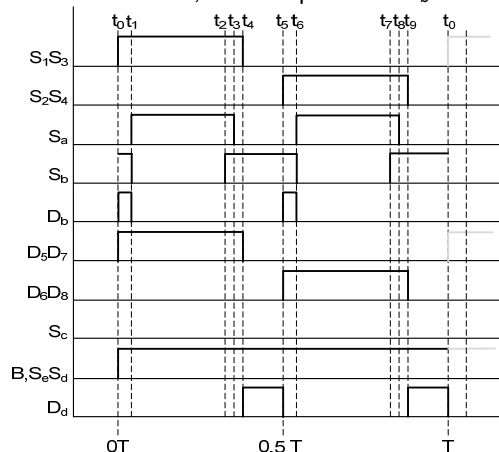


Fig.2. Operation diagram in boost mode

Stage "a" [ $t_0 \leq t < t_1$ ]: once the converter operates in steady state, the capacitor  $C_i$  has an initial charge, the instant  $t_0$  are connected  $S_1$  and  $S_3$ , so that the capacitor begins to discharge through the circuit formed by  $D_b$ ,  $S_1$ ,  $S_3$ , and the primary winding of the transformer. At this stage, at the converter output are conducting the diodes  $D_5$  and  $D_7$ , and is also activated IGBT  $S_d$  to filter the output current of the converter.

Step "b" [ $t_1 \leq t < t_2$ ]: at  $t_1$ ,  $S_a$  is connected and  $S_b$  is disconnected. The potential difference between the positive terminal of the DC source and the positive pole of  $C_i$ , can be regulated with  $R_1$  and  $R_2$  values, so that the connection and disconnection of  $S_a$  may occur close to 0 V, this can be seen in Fig. 8 Ch1, when  $S_a$  is connected, the diode  $D_b$  is reverse-biased, therefore the primary circuit is closed through  $S_a, S_1, L_1, S_3$ . The values of  $R_1$  and  $R_2$  regulate the voltage level of  $C_i$  and the charge and discharge currents of  $C_i$ .

Step "c" [ $t_2 \leq t < t_3$ ]: at  $t_2$ ,  $S_b$  is connected, so that the capacitor charge level rises during this stage, receiving charge from the battery. On the other side, the primary transformer remains connected to the battery through  $S_1, S_3$ . The output remains the same as in step b.

Step "d" [ $t_3 \leq t < t_4$ ]: at  $t_3$ ,  $S_a$  is turned off, the battery of the circuit stops supplying power to the transformer. The voltage in the capacitor  $C_i$  and the voltage in the coil  $L_1$  are added, resulting the partial discharge of the energy in the coil and in the capacitor, to maintain during this stage the flow of current through the primary windings, this current runs in the circuit  $C_i, D_b, S_1, B, S_3, L_1, C_i$ .

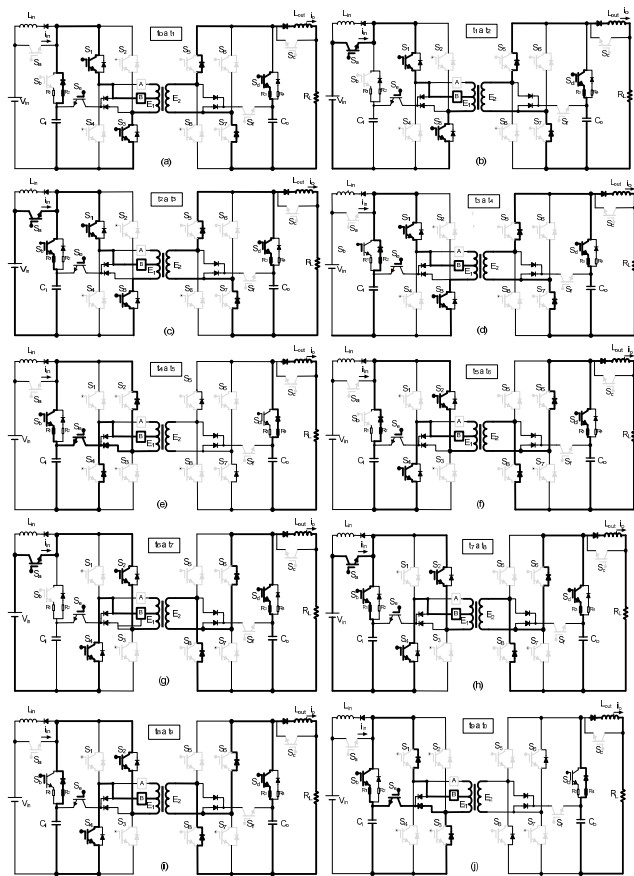


Fig.3. Steps in boost mode

Stage "e" [ $t_4 \leq t < t_5$ ]: at  $t_4$ ,  $S_1$  and  $S_3$  are disconnected. When this disconnection occurs, the primary winding of the transformer is starting the discharge process, this process occurs by two paths, one principal path through  $S_e$  and other through  $D_2, S_b, D_4$ . The energy that existed in the magnetic field of the coil is stored in the capacitor as load. The capacitor is charged at a level somewhat higher than  $V_{in}$  for the next stage. In the converter output circuit, part of the energy stored in  $L_{out}$  and in the capacitor is used for maintaining the flow of current through the load. This occurs through the circuit  $C_o, D_d, L_{out}, R_L$ . Also the energy exists in

the transformer's secondary windings, which is used to maintain flow through the load.

Stage "f" [ $t_5 \leq t < t_6$ ]: at  $t_5$ ,  $S_2, S_4$  are connected. These connections are done at zero current. When  $S_2, S_4$  are connected,  $C_i$  begins to discharge, initiating current flow in opposite direction in  $L_1$  through  $D_b$  and  $R_2$ . Furthermore in the output circuit, the circuit  $C_o, D_d, L_{out}, R_L$  retains current flow through the load  $R_L$ , but also starts the flow of current through  $D_6$  and  $D_8$ .

Step "g" [ $t_6 \leq t < t_7$ ]: at  $t_6$ ,  $S_a$  is switched on again, so that battery power is transmitted to the load. This stage works similar to step "b"; except that the IGBTs connected in input circuit are  $S_2$  y  $S_4$ . The diodes conducting in the output circuit are  $D_6$  y  $D_8$ , also the direction of the currents in the windings of the transformer is contrary to the currents in stage "b".

The steps "h" [ $t_7 \leq t < t_8$ ], "i" [ $t_8 \leq t < t_9$ ] and "j" [ $t_9 \leq t < t_{10}$ ] are similar to the steps "c", "d" and "e". The only difference between steps "h", "i" and step "c", "d" is that steps "h", "i" are connected by  $S_2$  and  $S_4$  in the input circuit and  $D_6$  and  $D_8$  are in the output circuit. Step "j" is different from the "e", since  $D_1$  and  $D_3$  are conducting in stage "j".

### Algorithm for the DSP and experimental results

The working algorithm of the bidirectional converter was implemented in MATLAB-Simulink and later the code was generated and debugged in a Spectrum Digital eZdsp™TMS320F2812 card, where the DSP is located.

In Fig. 4 the used Simulink model for programming the DSP is represented.

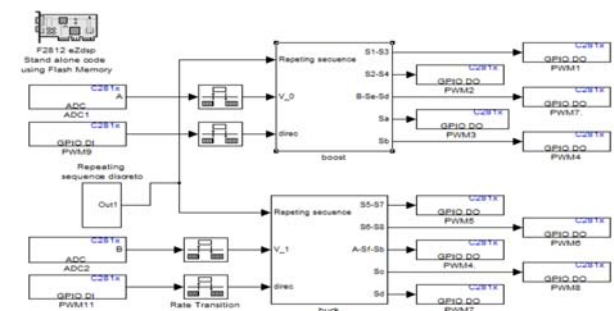


Fig.4. Model implemented in the Spectrum Digital card

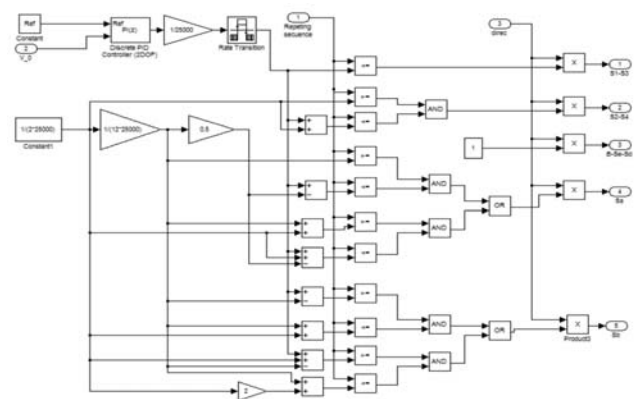


Fig.5. Inside of the "boost" block

This consists of a "boost" block that contains the switching algorithm when it is working in the boost mode, and a "buck" block containing the switching algorithm when it is working in the buck mode. The inputs PWM11 and PWM9 are responsible for activating the aforementioned blocks respectively, these blocks cannot work simultaneously.

Each of these blocks has an analog input for receiving information from the output voltage of the converter. Fig. 5 shows the inside of the “boost” block shown in Fig.4, in which a PI controller was used to stabilize the output voltage of the converter; this receives the feedback for the analog input ADC1. The inside of “buck” block is not shown, this is similar to inside of “boost” block, since the converter is symmetrical.

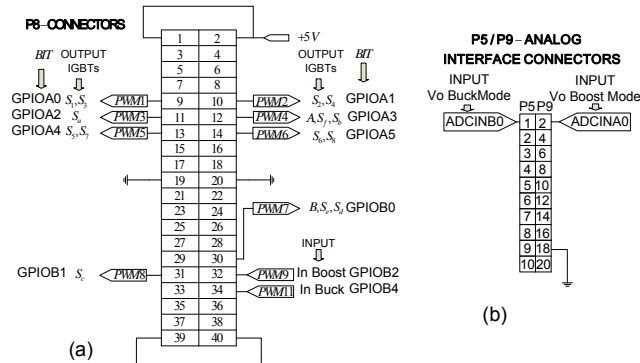


Fig. 6. Connection of the P8 and P5/P9 module of the Spectrum

Fig. 6 (a) shows the P8 module connection of the Digital Spectrum card. Each of the pins of the module is shown with the corresponding PWM signal, in the 'OUTPUT IGBTs' column, the converter IGBTs associated with each output are shown.

In columns “BIT”, the output configuration of the model in Matlab-Simulink can be found, associated with the corresponding output of module P8.

There are also two analog inputs, shown in Fig. 6b, they receive the feedback from the output signals of the converter in boost and buck modes. The configurations for these analog signals in Matlab-Simulink to implement the model are ADCINB0 and ADCINA0.

To test the algorithm, a laboratory prototype of a bi-directional converter has been built with an output of 600 W, 24V and with an input voltage of 12V,  $D_{nom}=0.33$ ,  $f_c=25\text{KHz}$  and  $\rho=0.91$ . Following elements have been used:

Three blocks of IGBTs (Infineon FS200R07A1E3) with encapsulation of 6 units at 250 A, 14 diodes (Omnirel OM4229RS) at 100A, 2 capacitors (Epcos MKP PEC DC 630 $\mu\text{F}$  47V). Two coils (Suesa) 12.7  $\mu\text{H}$  and 70 A, a 600 W transformer (Suesa) with two voltage taps and two turns ratios, as boost  $m=E_1/E_2=0.25=12/48$ , as buck  $m=E_2/E_1=1.5=24/16$ . Nine blocks of triggers (Elantec EL7242C) with two units per package, 4 25W resistors (ARCOR), 2 WH25H47 and two WH2510H.

The converter measurements were taken with a 1.5 $\Omega$  load resistor and an input of 12V from a battery. The obtained output was 24V, and whose voltage ripple can be seen in Fig. 9 Ch1. This ripple is close to 50mV. The current through the load was 16 A. The ripple value of that current is shown in Fig. 9 Ch2, is a value close to 34 mA. The current flowing through the branch  $C_o$  is shown in Fig. 9 Ch3. This stabilizes the voltage and the load current. The potential difference between battery and  $C_i$  can be seen in Fig.8 Ch1, being its oscillation range of 1.5 V., The voltage ripple in  $C_i$  is shown in Fig. 8 Ch2. This is 0.75 V on a value of 11.5 V. Fig.10 Ch3 shows the voltage at the ends of the primary windings of the transformer. It can be seen that the voltage spikes are not excessive with a maximum value of 21 V. This shows that there are no abrupt changes in resistance in the primary transformer circuit.

Fig 10 Ch1 shows the current at the output of battery. It has a peak value of 106 A and a triangular shape. It can be observed that the entire current is in positive zone, this

means that energy does not return from converter to source. Therefore the source is protected from possible voltage spikes that may occur in the converter.

Fig. 7 shows the transient voltage and current simulated with Matlab-Simulink. This transient can be eliminated when the capacitors  $C_i$  and  $C_o$  are charged before the converter starts working.

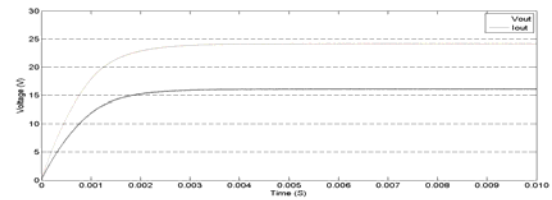


Fig. 7. Initial transient in load voltage and load current

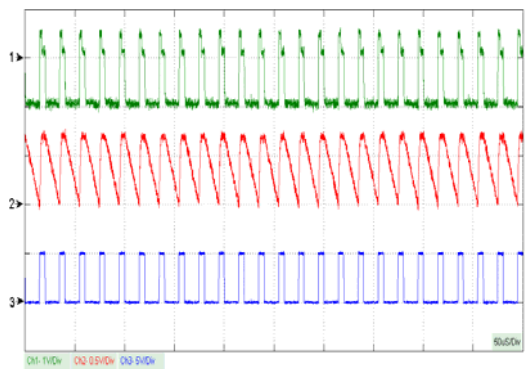


Fig. 8. (Ch1)- Potential difference between the positive pole  $V_{in}$  and the positive pole  $C_i$ . (Ch2)-  $C_i$  voltage ripple. (Ch3)-IGBT gate signal  $S_b$

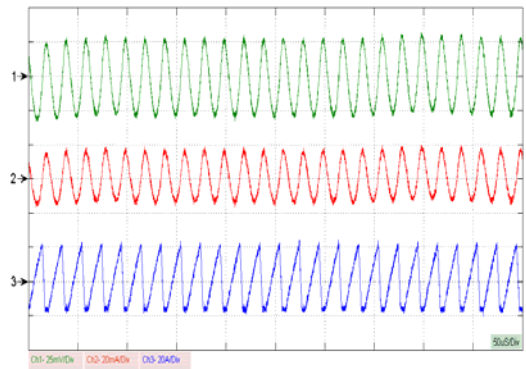


Fig 9. (Ch1)-load voltage ripple, (Ch2)-load current ripple, (Ch3)- Current in  $C_o$

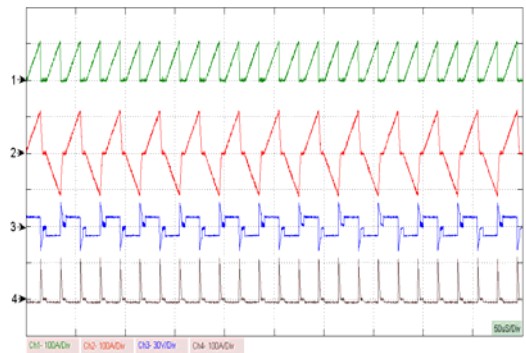


Fig 10.(Ch1)-Output current in the battery. (Ch2)-Current in transformer primary. (Ch3)-Voltage in transformer primary. (Ch4)- Current in capacitor branch  $C_i$



A display from CCS is shown in Fig 11. This demonstrates that the code has been successfully generated by Spectrum card. It can be observed that the construction of the project has not presented errors, warnings or remarks. Also the main file header can be shown.

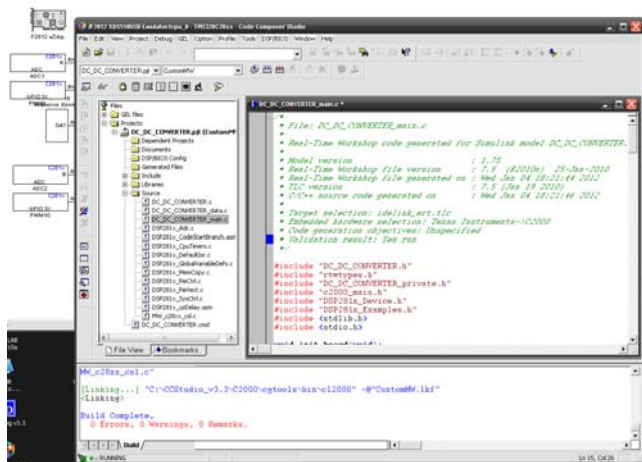


Fig 11. Display from CCS generating C code



Fig 12. Laboratory prototype of DC / DC bidirectional converter

## Conclusion

A new isolated bi-directional converter using a transformer with two voltage taps has been presented in this article. This converter can be used in devices at medium – high power using renewable energy sources. Design considerations and switching techniques have been reported. To verify the principle of operation, experimental results from a laboratory prototype of 600 W were shown working as a boost. The switching algorithm used was modeled in Matlab-Simulink to generate C code. This code was implemented in a Spectrum Digital eZdsp™TMS320F2812 card with DSP F2812, and was used to build the prototype. The design considerations can be applied to both bi-directional and unidirectional converter design.

## Nomenclature

$V_{in}$ ,  $V_o$ - Input voltage and output voltage.  
 $m$ ,- Transformer turns ratio.  
 $T, f_c$ ,- Commutation period and switching frequency.  
 $D$ ,- Duty cycle.  
 $E_1, E_2$ ,- Electromotive forces in primary and secondary windings.  
 $S_j, D_j$ ,- IGBT(s) and power diode circuit.  
 $R_L$  - Load resistance.  
 $C$  – Capacity of output filter capacitor.  
 $r_c$  – Capacitor equivalent series resistance of the filter.  
 $i_{in}$  - Input current.  
 $L_{out}, L_{in}$  – Inductances of filter coils.  
 $L_1$  – primary winding inductance.

$\Delta i_{L_{in}}, \Delta i_{L_{in}}$  - Current ripples in the coils of filters.  
 $\Delta V_{ab}$ – Ripple voltage between nodes “a” and “b”.  
 $M_{VDC}$ - Voltage transfer function.  
 $i_o$  - AC component of output current.  
 $\Delta i_o, \Delta i$  - Current ripples in the filter coil and node “a”.  
 $I_o$  - DC component of output current.  
 $\rho$ - Efficiency of converter.

## REFERENCES

- [1] Kasa N., Harada Y., Ida T., and Bhat A. K. S., Zero-current transitions converters for independent small scale power network system using lower power wind turbines, *Proc. IEEE Int. Symp. Power Electron., Electric Drives, Autom. Motion*, (2006), May, 1206–1210
- [2] Swingler A. D. and Dunford W. G., Development of a bidirectional DC/DC converter for inverter/charger applications with consideration paid to large signal operation and quasi-linear digital control, *Proc. IEEE PESC*, (2002), Jun., 961–966.
- [3] Lai J. and Nelson D. J., Energy management power converters in hybrid electric and fuel cell vehicles, *Proc. IEEE*, 95 (2007) Apr., no. 4, 766–777.
- [4] Ortega M., Jurado F., and Carpio J., Control of indirect matrix converter with bidirectional output stage for micro-turbine, *IET Power Electronics*, No.7, 5 (2012).
- [5] Peng F. Z., Li H., Su G.-J., and Lawler J. S., A new ZVS bidirectional dc–dc converter for fuel cell and battery application,” *IEEE Trans. Power Electron.*, 19 (2004), No. 1, 54–65.
- [6] Chong B. V. P., Zhang L. and Dehghani A., Modeling & control of a bidirectional converter for a stand-alone photovoltaic power plant, *Proc. Eur. Conf. Power Electron. Appl.* (2007), Sep., 1–10.
- [7] Hua C.-C., Chuang Ch.-W., Wu Ch.-W., and Chuang D.-J., Design and implementation of a digital high-performance photovoltaic lighting system, *Proc. ICIEA* (2007), May, 2583–2588.
- [8] Mohan N., Undeland T. M. and Robbins W. P., *Power Electronics: Converters, Applications and Design*. (2003) New York: Wiley.
- [9] De Doncker R. W., Divan D. M., and Kheraluwala M. H., A three phase soft-switched high power density dc/dc converter for high power application, *IEEE Trans. Ind. Appl.*, 27 (1991) No. 1, 63–73.
- [10] Kheraluwala M. H., Gascoigne R., Divan D.M., and Baumann E., Performance characterization of a high power dual active bridge DC-to-DC converter, *IEEE Trans. Ind. Appl.*, 28 (1992), No. 6, 1294–1301.
- [11] Xiao H. and Xie S., A ZVS bidirectional DC-DC converter with phaseshift plus PWM control scheme, *IEEE Trans. Power Electron.*, 23 (2008) No. 2, 813–823.
- [12] Bai H. and Mi C., Eliminate reactive power and increase system efficiency of isolated bidirectional dual-active-bridge DC-DC converters using novel dual-phase-shift control, *IEEE Trans. Power Electron.*, 23 (2008), No. 6, 2905–2814.

**Authors:** Prof. Dr. Manuel Ortega. Department of Electrical Engineering, Escuela Politecnica Superior de Linares, University of Jaén, 23700 Linares, Spain, E-mail: maortega@ujaen.es.  
 Juan Carlos Lopez, Construcciones y Auxiliar de Ferrocarriles, Linares, 23700, E-mail: JCLopez@cfsantana.net  
 Prof. Dr. Francisco Jurado. Department of Electrical Engineering, Escuela Politecnica Superior de Linares, University of Jaén, 23700 Linares, Spain, E-mail: fjurado@ujaen.es.

The correspondence address is:  
 e-mail: fjurado@ujaen.es